Hindawi
Advances in High Energy Physics
Volume 2017, Article ID 4693213, 9 pages
https://doi.org/10.1155/2017/4693213

Research Article

Searches for the Anomalous FCNC Top-Higgs Couplings with Polarized Electron Beam at the LHeC

XiaoJuan Wang, Hao Sun, and Xuan Luo

Institute of Theoretical Physics, School of Physics & Optoelectronic Technology, Dalian University of Technology, No. 2 Linggong Road, Dalian, Liaoning 116024, China

Correspondence should be addressed to Hao Sun; haosun@dlut.edu.cn

Received 29 September 2016; Revised 2 December 2016; Accepted 4 January 2017; Published 16 March 2017

Academic Editor: Burak Bilki

We study the single top and Higgs associated production $e^- p \to \nu_e \bar{t} \to \nu_e h\bar{q}(h \to b\bar{b})$ in the top-Higgs FCNC couplings at the LHeC with the electron beam energy of $E_e = 60$ GeV and $E_e = 120$ GeV and combination of a 7 TeV and 50 TeV proton beam. With the possibility of e-beam polarization ($p_e = 0, \pm 0.6$), we distinct the cut-based method and the multivariate analysis- (MVA-) based method and compare with the current experimental and theoretical limits. It is shown that the branching ratio Br($t \to uh$) can be probed to 0.113 (0.093%), 0.071 (0.057%), 0.030 (0.022%), and 0.024 (0.019%) with the cut-based (MVA-based) analysis at (E_p, E_e) = (7 TeV, 60 GeV), (E_p, E_e) = (7 TeV, 120 GeV), (E_p, E_e) = (50 TeV, 60 GeV), and (E_p, E_e) = (50 TeV, 120 GeV) beam energy and 1σ level. With the possibility of e-beam polarization, the expected limits can be probed down to 0.090 (0.073%), 0.056 (0.045%), 0.024 (0.018%), and 0.019 (0.015%), respectively.

1. Introduction

The Large Hadron Electron Collider (LHeC) is the second electron-hadron collider following HERA [1]. With remarkable higher energy and luminosity, the LHeC is a major step towards understanding the Higgs physics and QCD. For the LHeC colliding energy, the 7 TeV proton beam at the LHC as well as the 50 TeV proton beam at the future FCC-he [2] and a new 60 GeV electron beam [1] are envisaged. To probe new physics, the anomalous flavor changing neutral current (FCNC) Yukawa interactions, between the top-Higgs and either an up or charm quark, would provide a clear signal. The SM Lagrangian can be extended by the following terms:

$$\mathscr{L} = \kappa_{tuh}\bar{t}uh + \kappa_{tch}\bar{t}ch + \text{h.c.}, \tag{1}$$

where the real parameters κ_{tuh} and κ_{tch} denote the FCNC couplings of the Higgs to up-type quarks. The total decay width of the top quark Γ_t is

$$\Gamma_t = \Gamma^{\text{SM}}_{t\to W^- b} + \Gamma_{t\to ch} + \Gamma_{t\to uh}, \tag{2}$$

where the decay width $\Gamma^{\text{SM}}_{t\to W^- b}$ and $\Gamma_{t\to u(c)h}$ can be found in [3, 4], respectively. Thus, the branching ratio for $t \to u(c)h$ can be approximately given by

$$\begin{aligned}\text{Br}\,(t \longrightarrow u\,(c)\,h) &= \frac{\kappa^2_{tu(c)h}}{\sqrt{2}G_F m_t^2}\frac{\left(1-\tau_h^2\right)^2}{\left(1-\tau_W^2\right)^2\left(1+2\tau_W^2\right)} \\ &\approx 0.512\kappa^2_{tu(c)h},\end{aligned} \tag{3}$$

where G_F is the Fermi constant and $\tau_W = m_W/m_t$. The W boson and top quark masses are chosen to be $m_W = 79.82$ GeV and $m_t = 173.2$ GeV, respectively.

Up to now, the investigation of $t \to qh$ anomalous couplings has been experimented by many groups, which gives the strong limits on the top-Higgs FCNC couplings. For instance, according to the ATLAS and CMS collaborations, the upper limits of Br($t \to qh$) < 0.79% [5, 6] and Br($t \to qh$) < 0.45% [7] have been set at 95% confidence level (CL). At one-loop level, the $D^0 - \overline{D^0}$ mixing observable can receive sizeable contributions with such an unvanishing flavor violating tqH coupling [8]. Using data observed on $D^0 - \overline{D^0}$,

Table 1: The results from different experimental and phenomenological channels.

Channels	Data set	Limits
$t\bar{t} \to Wbqh \to \ell\nu b\gamma\gamma q$	ATLAS, 4.7 (20.3) fb^{-1} @ 7 (8) TeV	Br($t \to qh$) < 0.79% [5, 6]
$t\bar{t} \to Wbqh \to \ell\nu b\gamma\gamma q$	CMS, 19.5 fb^{-1} @ 8 TeV	Br($t \to uh$) < 0.45% [7]
$D^0 - \overline{D^0}$ mixing data	—	Br($t \to qh$) < 0.5% [8]
$Z \to c\bar{c}$ and EW observables	—	Br($t \to qh$) < 0.21% [9]
$Wt \to Whq \to \ell\nu b\gamma\gamma q$	LHC, 3000 fb^{-1} @ 14 TeV, 3σ	Br($t \to qh$) < 0.24% [10]
$t\bar{t} \to Wbqh \to \ell\nu b\gamma\gamma q$	LHC, 3000 fb^{-1} @ 14 TeV	Br($t \to uh$) < 0.23% [11]
$t\bar{t} \to tqh \to \ell\nu bb\bar{b}q$	ILC, 3000 fb^{-1} @ 500 GeV	Br($t \to qh$) < 0.112% [12]
$th \to \ell\nu b\tau^+\tau^-$	LHC, 100 fb^{-1} @ 13 TeV	Br($t \to uh$) < 0.15% [13]
$th \to \ell\nu b\ell^+\ell^- X$	LHC, 100 fb^{-1} @ 13 TeV	Br($t \to uh$) < 0.22% [13]
$th \to jjbb\bar{b}$	LHC, 100 fb^{-1} @ 13 TeV	Br($t \to uh$) < 0.36% [13]

the upper limit of Br($t \to qh$) < 5×10^{-3} can be achieved. Furthermore, through $Z \to c\bar{c}$ decay and electroweak observables, the upper limit of Br($t \to qh$) < 0.21% [9] can be obtained.

On the other hand, based on the experimental data, many phenomenological studies are performed from different channels. For instance, [10] found that the branching ratios Br($t \to qh$) can be probed to 0.24% at 3σ level at 14 TeV LHC with integrated luminosity of 3000 fb^{-1} through the process $Wt \to Whq \to \ell\nu b\gamma\gamma q$. Reference [11] explored the top-Higgs FCNC couplings through $t\bar{t} \to Wbqh \to \ell\nu b\gamma\gamma q$ and found that the branching ratios Br($t \to uh$) can be probed to 0.23% at 3σ sensitivity at 14 TeV LHC with = 3000 fb^{-1}. And [12] obtained Br($t \to qh$) to be 0.112% based on the process of $t\bar{t} \to tqh \to \ell\nu bb\bar{b}q$. The process of $th \to \ell\nu b\tau^+\tau^-$ has been studied in [13] and the authors therein estimated the upper limits of Br($t \to uh$) < 0.15% at 100 fb^{-1} of 13 TeV data for multilepton searches. The results from different experiments and theoretical channels are summarized in Table 1.

In this study, we examined $e^- p \to \nu_e \bar{t} \to \nu_e h\overline{q}$ at the LHeC, where the Higgs boson decays to $b\bar{b}$ at 7 (50) TeV with 60 (120) GeV electron beam and 1000 fb^{-1} integrated luminosity. The possibility of e-beam polarization is also considered. The Feynman diagram is plotted in Figure 1. The main backgrounds which yield the same or similar final states to the signal are listed as follows:

$$
\begin{aligned}
&e^- p \longrightarrow \nu_e \left(\bar{t} \longrightarrow (W^- \longrightarrow jj)\,\bar{b}\right),\\
&e^- p \longrightarrow e^- jjj,\\
&e^- p \longrightarrow \nu_e jjj,\\
&e^- p \longrightarrow \nu_e \left(h \longrightarrow b\bar{b}\right) j,\\
&e^- p \longrightarrow \nu_e \left(z \longrightarrow b\bar{b}\right) j,
\end{aligned}
\tag{4}
$$

where $j = g, u, \overline{u}, d, \overline{d}, c, \overline{c}, s, \overline{s}, b$, and $\overline{b}$ if possible. Notice that $e^- p \to e^- jjj$ is the neutral current multijet QCD background, and all the others belong to charged current (CC) productions. For the single top background $e^- p \to \nu_e(\bar{t} \to (W^- \to jj)\bar{b})$, the produced top quark will decay to a W boson and a b-jet. The W boson continues to decay to non-b-jet final states, which might be mistagged as a b-jet. With the same final states, $e^- p \to \nu_e(h \to b\bar{b})\, j$ and $e^- p \to \nu_e(z \to b\bar{b})\, j$ are the irreducible backgrounds corresponding to associated Higgs jet and Z jet which contain three QED couplings. $e^- p \to \nu_e jjj$ is the CC multijet QCD background. Similar to the single top background, misidentification of one or more of the final state light jets to b-jet makes this process a reducible background.

2. Tools and Method

During the simulation, we first extract the Feynman Rules by using the FeynRules package [14] and generate the event with MadGraph@NLO [15]. PYTHIA6.4 [16] was set to solve the initial and final state parton shower, hadronization, heavy hadron decays, and so forth. We use CTEQ6L [17, 18] as the parton distribution function and set the renormalization and factorization scale to be $\mu_r = \mu_f$. We take the input heavy particle masses as $m_h = 125.7$ GeV, $m_t = 173.2$ GeV, $m_Z = 91.1876$ GeV, and $m_W = 79.82$ GeV, respectively. We employ the following basic preselections cuts to select the events:

$$
\begin{aligned}
&\not{E}_T^{\text{missing}} \geq 15\ \text{GeV},\\
&p_T^{k_0} \geq 15\ \text{GeV}, \quad k_0 = j, b, \ell,\\
&\left|\eta^j\right| < 5,\\
&\left|\eta^b\right| < 5,\\
&\left|\eta^\ell\right| \leq 3,\\
&\Delta R\left(k_1 k_2\right) > 0.4, \quad k_1 k_2 = jj, j\ell, jb, bb, b\ell,
\end{aligned}
\tag{5}
$$

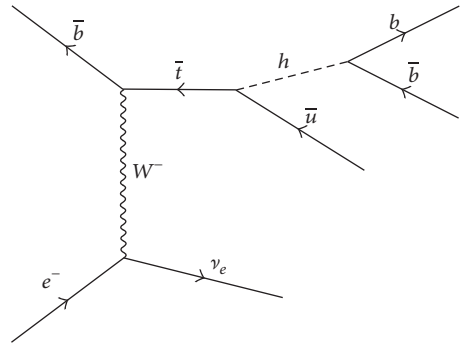

FIGURE 1: Feynman diagram for the partonic process $e^-\bar{b} \to \nu_e \bar{t} \to \nu_e h\bar{q} \to \nu_e b\bar{b}\bar{q}$ at the LHeC through flavor changing top-Higgs interactions.

where $\Delta R = \sqrt{\Delta\Phi^2 + \Delta\eta^2}$ is the separation with $\Delta\eta$ and $\Delta\Phi$ in the rapidity-azimuth plane and $p_T^{\text{jet},b,\ell}$ and $|\eta^{\text{jet},b,\ell}|$ are the transverse momentum and the pseudorapidity of jets, b-jets, and leptons, while $\not{E}_T^{\text{missing}}$ is the missing transverse momentum. Then we adopt a cut-based method and a multivariate analysis- (MVA-) based method for signal and background analysis, respectively.

2.1. Cut-Based Method. In order to distinguish between signal-related events and background-related events as much as possible, we set a series of cuts. We list all the cut-based selections here:

(i) Cut 1: the basic preselection cuts

(ii) Cut 2: the selection $e^- p \to \not{E}_T^{\text{missing}} + 0\ \ell + \geq 3$ jets, (with at least 2 tagged b-jets)

(iii) Cut 3: missing transverse energy $\not{E}_T^{\text{missing}} > 20\,\text{GeV}$

(iv) Cut 4: the reconstructed top quark mass window $m_t \in [148\,\text{GeV}, 178\,\text{GeV}]$

(v) Cut 5: the reconstructed W boson mass window $m_W < 50\,\text{GeV}$ or $m_W > 90\,\text{GeV}$

(vi) Cut 6: the reconstructed Z boson mass window $m_Z < 55\,\text{GeV}$ or $m_Z > 95\,\text{GeV}$

(vii) Cut 7: the reconstructed Higgs mass window $m_h \in [100\,\text{GeV}, 130\,\text{GeV}]$

2.2. MVA-Based Method. We implemented the MVA method using the Root Toolkit for Multivariate Analysis (TMVA) [19]. After cut 1, cut 2, and cut 3, we especially select several input variables to discriminate the signal and background events, thus resulting in better signal significance. Specifically, we define a set of totally 44 kinematic variables and choose the most effective ones for Boosted Decision Trees (BDT) training, which are the b-jet number ($N_{b\text{jet}}$), the separation in the Φ-η plane between jets ($\Delta R^{B_1B_2}$, $\Delta R^{B_1J_1}$), the difference in azimuthal angle between jets ($\Delta\Phi^{B_1B_2}$, $\Delta\Phi^{B_1J_1}$), the transverse momentum of the jet ($p_T^{J_1}$), and the difference in $|\eta|$ within Higgs jet system ($\Delta\eta^{hJ_1}$). It is worth noting that e-beam polarization is considered in both cut-based method and MVA-based method.

3. Results

In Figure 2 ((60) GeV) and Figure 3 ((120) GeV), we show the dependence of the cross section σ on the top-Higgs FCNC couplings κ_{tqh} at $E_e = 60$ (120) GeV with $p_e = \pm 0.6$ electron beam polarization and combination of a 7 (50) GeV proton beam for three different cases: (I) $\kappa_{tqh} = \kappa_{tuh}, \kappa_{tch} = 0$, (II) $\kappa_{tqh} = \kappa_{tch}, \kappa_{tuh} = 0$, and (III) $\kappa_{tqh} = \kappa_{tuh} = \kappa_{tch}$. Obviously, the cross section of $\kappa_{tqh} = 0.1$ can be 100 times larger than that of $\kappa_{tqh} = 0.01$, and the cross section of 50 TeV can be 9.1 (6.6) times larger than that of 7 TeV with a 60 (120) GeV electron beam. We also find that the cross sections between polarized and unpolarized electron beam cases are related as $\sigma_{e_r^-} = \sigma_{e_0^-} \cdot (1 - p_{e_r^-})$ and $\sigma_{e_l^-} + \sigma_{e_r^-} = 2\sigma_{e_0^-}$, independent of being case I, case II, or caseIII. Here $\sigma_{e_r^-}$, $\sigma_{e_l^-}$, and $\sigma_{e_0^-}$ represent the right, left, and without electron beam polarization, respectively.

The cross section of the signal and backgrounds (in units of fb) are summarized in Table 2 (cut-based method) and Table 3 (MVA-based method). From these tables, we calculate the signal significance $S/\sqrt{S+B}$ as 4.191 (15.341) and 6.652 (19.236) for 7 and 50 TeV by cut-based method and 4.921 (16.934) and 7.874 (20.785) by MVA-based method after imposing all the relevant event selections (only the first three selections in MVA-based method), respectively. Obviously, compared to the cut-based method, the MVA-based method can get better signal significance. As expected, with the $p_2 = -0.6$ e-beam polarization, the results are improved as 5.302 (19.404) and 8.414 (24.335) for cut-based method and 6.224 (21.420) and 9.960 (26.291) for MVA-based method. In addition to effective cuts, enhancing the b-tagging efficiency together with reducing the jet misidentification rates is one of the other ways to improve the signal significance. It is confirmed that the signal significance can be increased from 4.191, 6.652, 15.341, and 19.238 to 8.366, 13.840, 33.750, and 44.154 with $\epsilon_b = 80\%$, $\epsilon_c = 1\%$, and $\epsilon_{\text{light}} = 0.1\%$ with the same value of the input parameters and kinematic cuts.

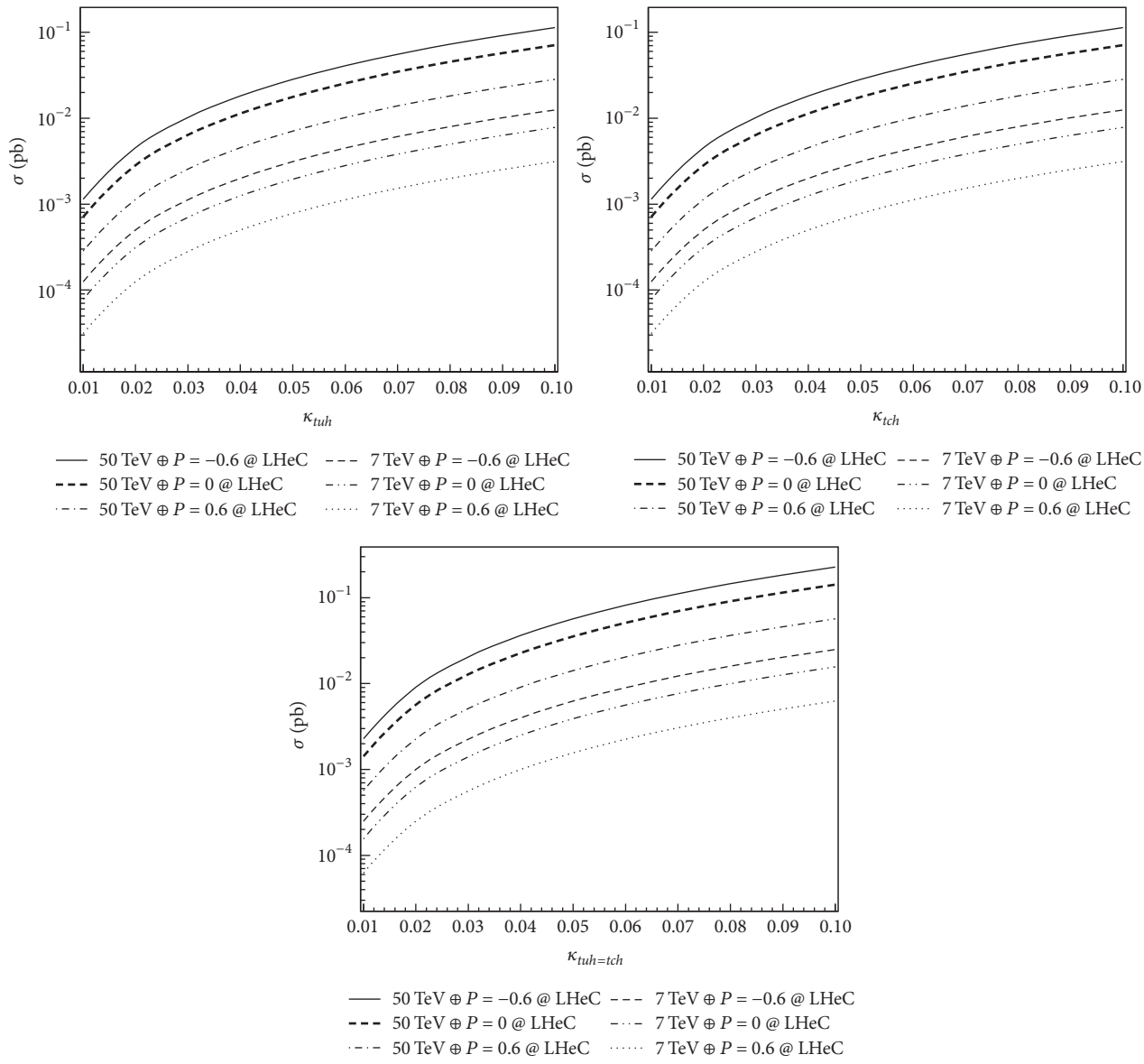

FIGURE 2: The cross sections σ_{tqh} on the top-Higgs FCNC couplings κ_{tqh} at the 7 (50) TeV and 60 GeV LHeC with e-beam polarization $p_e = 0, \pm 0.6$.

In order to estimate the sensitivity to the anomalous tqH couplings, we used chi-square (χ^2) function [20, 21]:

$$\chi^2 = \left(\frac{\sigma_{\text{tot}} - \sigma_B}{\sigma_B \delta} \right)^2, \tag{6}$$

where σ_{tot} is the total cross section and δ is the statistical error. In Figure 4 (cut-based analysis) and Figure 5 (MVA-based analysis) [19], we plot the contours of 1σ limits to κ_{tqH} at 7 (50) GeV LHeC and 60 (120) GeV electron beam with different polarization. The red, blue, and black curves represent the 0.6, −0.6, and without electron beam polarization. From these figures, we can see that the branching ratio $\text{Br}(t \to uh)$ can be probed to 0.113 (0.093%), 0.071 (0.057%), 0.030 (0.022%), and 0.024 (0.019%) with the cut-based (MVA-based) analysis at $(E_p, E_e) = (7\text{ TeV}, 60\text{ GeV})$, $(E_p, E_e) = (7\text{ TeV}, 120\text{ GeV})$, $(E_p, E_e) = (50\text{ TeV}, 60\text{ GeV})$, and $(E_p, E_e) = (50\text{ TeV}, 120\text{ GeV})$ beam energy. As expected, the MVA-based method has a great advantage and also the 50 TeV high energy can get better results compared to the 7 TeV ones. Furthermore, it is clear that the limits can be probed down to 0.090 (0.073%), 0.056 (0.045%), 0.024 (0.018%), and 0.019 (0.015%) with the e-beam polarization of $p_2 = -0.6$.

Finally, we give precise integrated luminosity ($\mathscr{L}$) corresponding to the critical limits obtained by the experimental results (Table 4) and other phenomenological studies

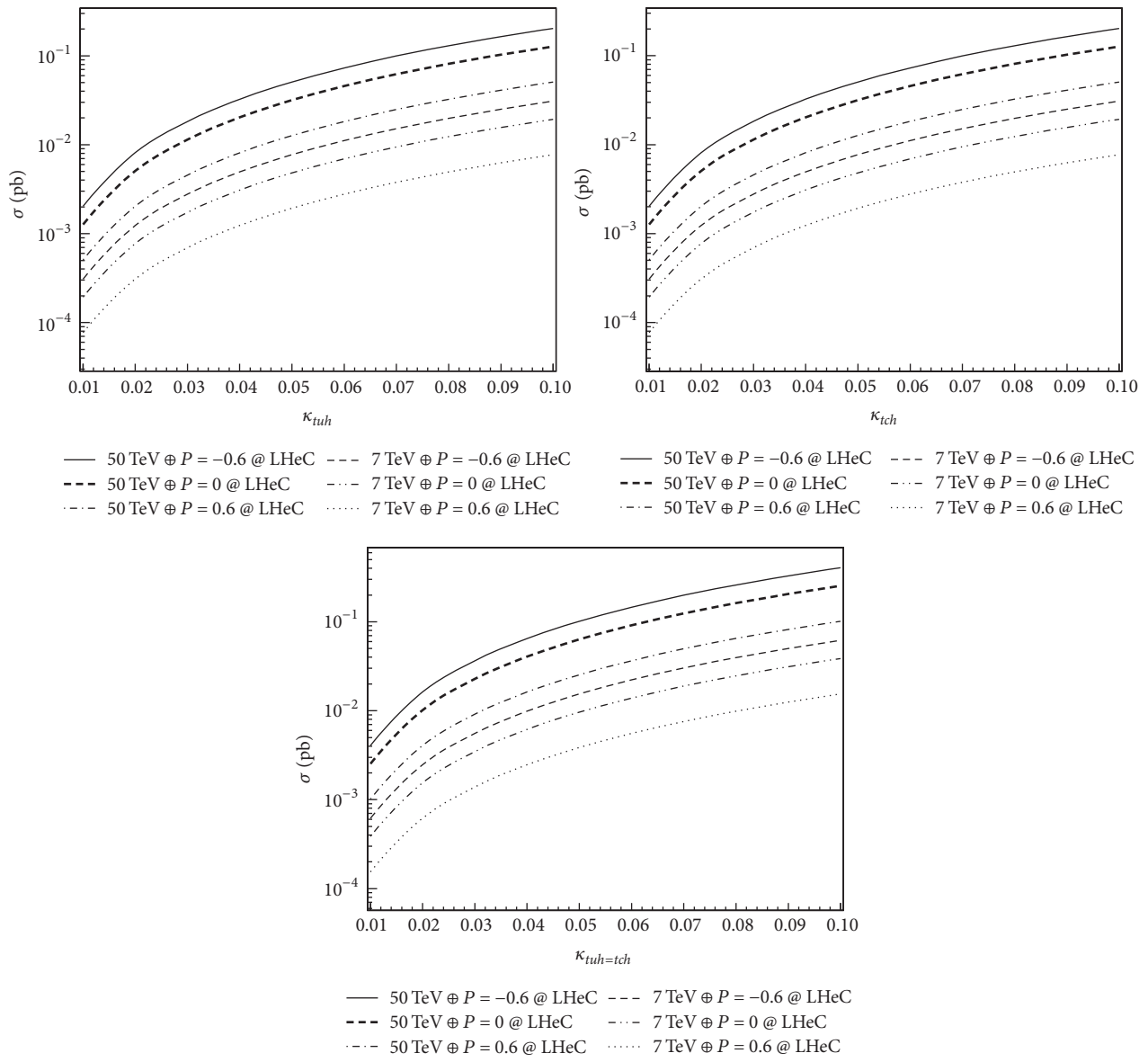

Figure 3: The same as Figure 2 but for E_e = 120 GeV.

(Table 5). With the e-beam polarization $p_2 = -0.6$, $\mathscr{L}$ needed to get the upper bounds on Br($t \to qh$) is reduced significantly. A detailed comparison between the LHeC collider(s) and the LHC or linear colliders is given.

4. Conclusion

In this paper, we investigated the anomalous FCNC Yukawa interactions between the top quark, the Higgs boson, and either an up or charm quark with a channel $e^- p \to \nu_e \bar{t} \to \nu_e h\bar{q}(h \to b\bar{b})$ at the LHeC. The signal significance $S/\sqrt{S+B}$ can be obtained as 4.191 (4.921), 6.652 (7.874), 15.341 (16.934), and 19.238 (20.785) with the cut-based (MVA-based) method at (E_p, E_e) = (7 TeV, 60 GeV), (E_p, E_e) = (7 TeV, 120 GeV), (E_p, E_e) = (50 TeV, 60 GeV), and (E_p, E_e) = (50 TeV, 120 GeV). Similarly, our results show that the branching ratio Br($t \to uh$) can be probed to 0.113 (0.093%), 0.071 (0.057%), 0.030 (0.022%), and 0.024 (0.019%), and with the e-beam polarization $p_2 = -0.6$, the expected limits can be greatly reduced. Finally, a detailed comparison between our study and the critical limits obtained by the experiments and other phenomenological studies is shown. We thus give an overview of the search potential on the anomalous top-Higgs couplings with polarized electron beam at the LHeC.

Conflicts of Interest

The authors declare that they have no Conflicts of interest.

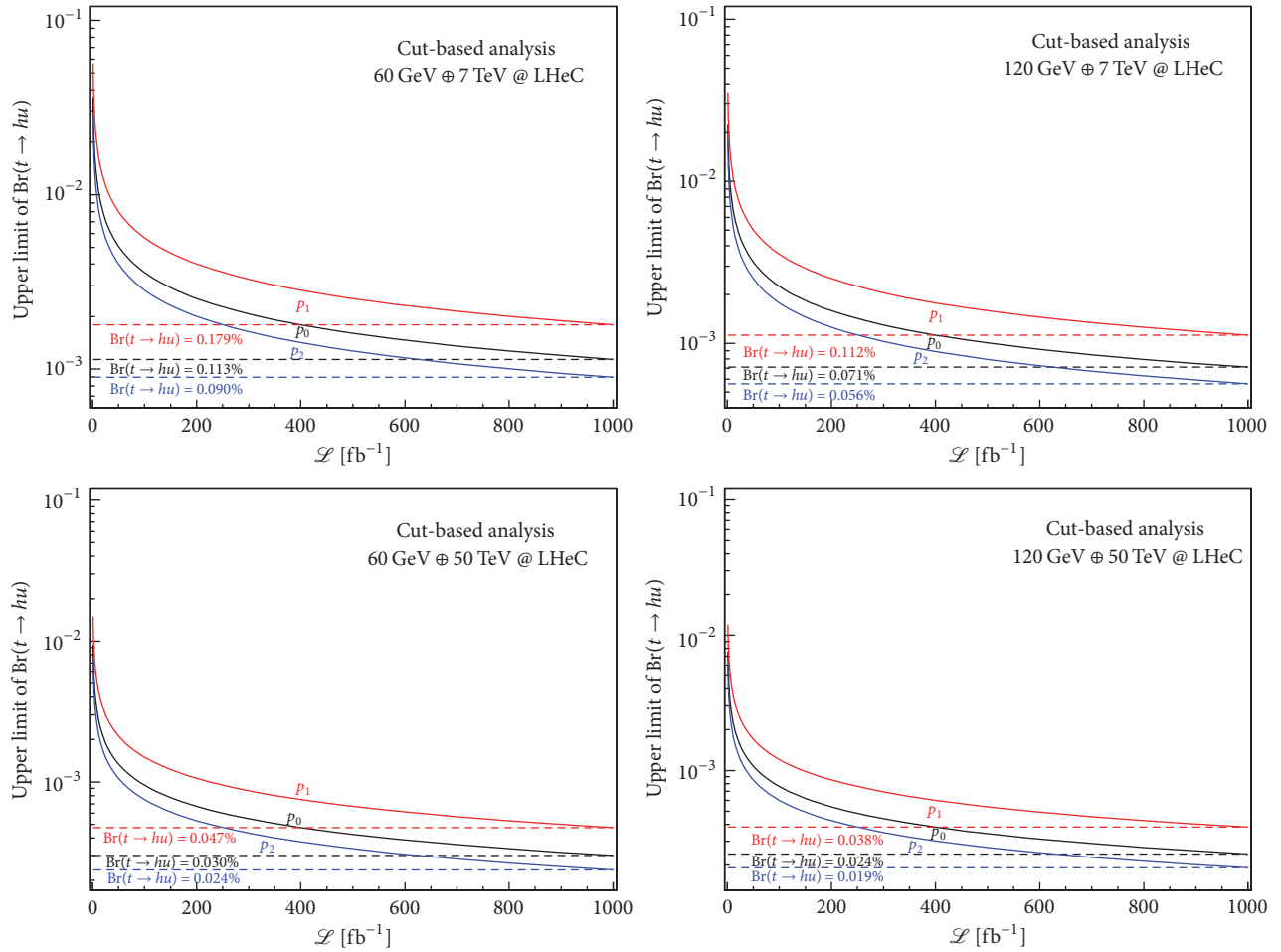

FIGURE 4: The upper limit from cut-based method at 1σ level at 7 (50) GeV LHeC with 60 (120) GeV electron beam. The red, blue, and black curves represent the 0.6, −0.6, and without electron beam polarization.

TABLE 2: Expected cross sections after all the selections for signal and backgrounds at the LHeC with integrated luminosity of 1000 fb^{-1}, b-tagging efficiency $\epsilon_b = 60\%$, jet misidentification rates $\epsilon_c = 10\%$, and $\epsilon_{\text{light}} = 1\%$ by cut-based method. In particular, we select e-beam polarization as $p_0 = 0$, $p_1 = 0.6$, and $p_2 = -0.6$.

	S	B	SS
60 GeV ⊕ 7 TeV @ LHeC			
p_0	0.14	0.93	4.191
p_1	0.05	0.37	2.651
p_2	0.22	1.49	5.302
120 GeV ⊕ 7 TeV @ LHeC			
p_0	0.32	1.98	6.652
p_1	0.13	0.79	4.207
p_2	0.51	3.16	8.414
60 GeV ⊕ 50 TeV @ LHeC			
p_0	1.29	5.80	15.341
p_1	0.52	2.32	9.702
p_2	2.07	9.28	19.404
120 GeV ⊕ 50 TeV @ LHeC			
p_0	2.14	10.26	19.238
p_1	0.86	4.10	12.167
p_2	3.43	16.42	24.335

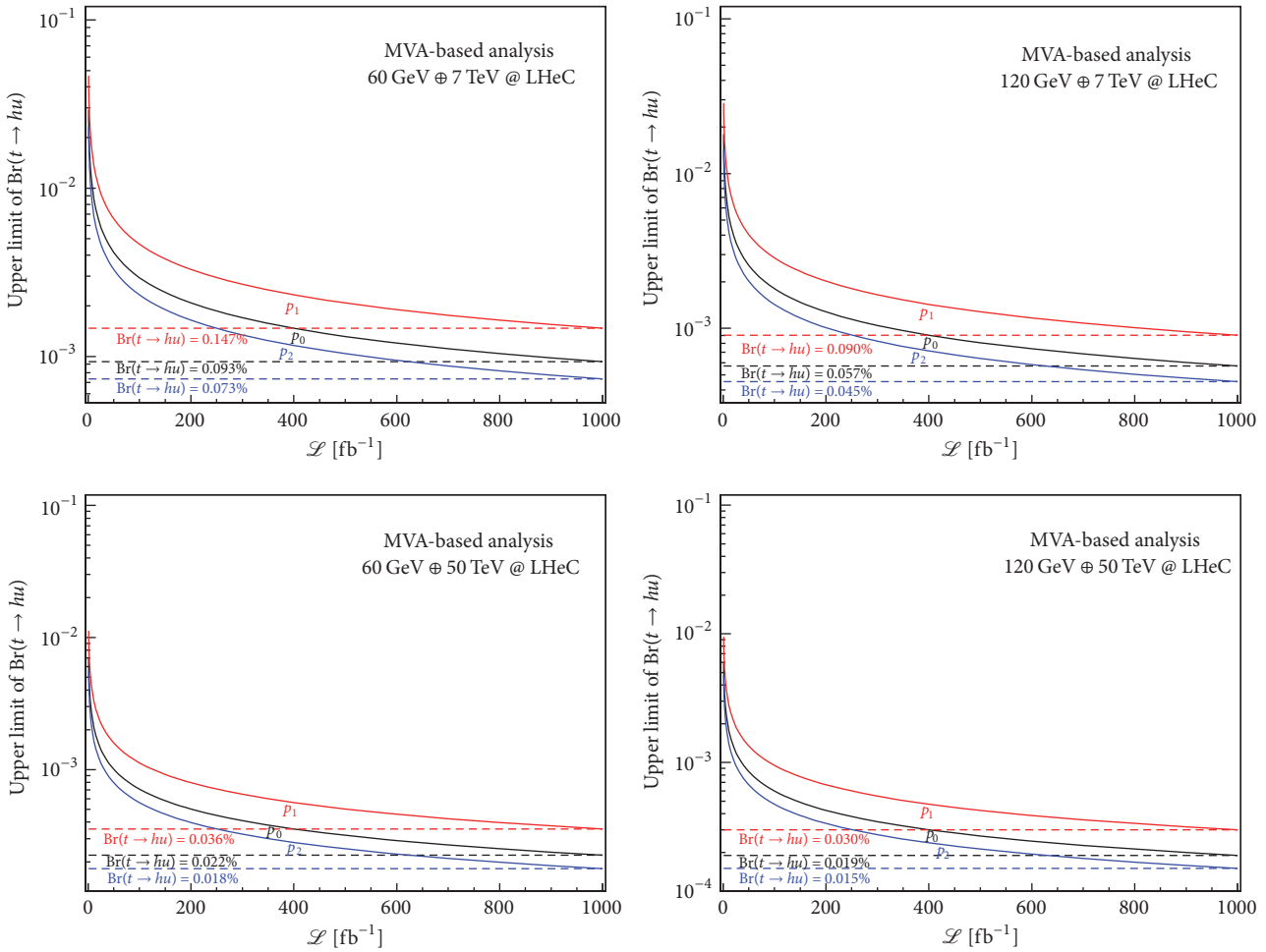

Figure 5: The same as Figure 4 but for MVA.

Table 3: The same as Table 2 but for MVA-based method. We select e-beam polarization as $p_0 = 0$, $p_1 = 0.6$, and $p_2 = -0.6$.

	S	B	SS
60 GeV ⊕ 7 TeV @ LHeC			
p_0	0.125	0.520	4.921
p_1	0.050	0.208	3.112
p_2	0.200	0.833	6.224
120 GeV ⊕ 7 TeV @ LHeC			
p_0	0.281	0.992	7.874
p_1	0.112	0.397	4.980
p_2	0.450	1.588	9.960
60 GeV ⊕ 50 TeV @ LHeC			
p_0	0.652	0.830	16.934
p_1	0.261	0.332	10.710
p_2	1.043	1.328	21.420
120 GeV ⊕ 50 TeV@ LHeC			
p_0	1.082	1.629	20.785
p_1	0.433	0.652	13.145
p_2	1.732	2.606	26.291

Table 4: The integrated luminosity ($\mathscr{L}$) needed to get the upper bounds on Br($t \to qh$) at 95% CL obtained from the experiments. Both the cut- (MVA-) based results and 1σ (2σ) limits with e-beam polarization are presented.

Channels and limits	Method	$\mathscr{L}$ [fb^{-1}]$_{1\sigma}$			$\mathscr{L}$ [fb^{-1}]$_{2\sigma}$		
		p_0	p_1	p_2	p_0	p_1	p_2
$t\bar{t} \to Wbqh \to \ell\nu b\gamma\gamma q$ ATLAS, 4.7 (20.3) fb^{-1} @ 7 (8) TeV Br($t \to qh$) < 0.79% [5, 6]	Cut MVA	0.93 0.58	2.32 1.44	0.58 0.36	3.60 2.24	9.00 5.60	2.25 1.40
$t\bar{t} \to Wbqh \to \ell\nu b\gamma\gamma q$ CMS, 19.5 fb^{-1} @ 8 TeV Br($t \to uh$) < 0.45% [7]	Cut MVA	2.86 1.78	7.15 4.45	1.79 1.11	11.10 6.91	27.76 17.27	6.94 4.32
$D^0 - \overline{D^0}$ mixing data Br($t \to qh$) < 0.5% [8]	Cut MVA	2.32 1.44	5.79 3.60	1.45 0.90	8.99 5.60	22.48 13.99	5.62 3.50
$Z \to c\bar{c}$ and EW observables Br($t \to qh$) < 0.21% [9]	Cut MVA	13.13 8.17	32.83 20.43	8.21 5.11	51.01 31.74	127.53 79.35	31.88 19.84

Table 5: The same as Table 4 but for some other phenomenological studies.

Channels and limits	Method	$\mathscr{L}$ [fb^{-1}]$_{1\sigma}$			$\mathscr{L}$ [fb^{-1}]$_{2\sigma}$		
		p_0	p_1	p_2	p_0	p_1	p_2
Wt $\to Whq \to \ell\nu b\gamma\gamma q$ LHC, 3000 fb^{-1} @ 14 TeV 3σ, Br($t \to qh$) < 0.24% [10]	Cut MVA	10.05 6.26	25.14 15.64	6.28 3.91	39.05 24.30	97.63 60.75	24.41 15.19
$t\bar{t} \to Wbqh \to \ell\nu b\gamma\gamma q$ LHC, 3000 fb^{-1} @ 14 TeV Br($t \to uh$) < 0.23% [11]	Cut MVA	10.95 6.81	27.37 17.03	6.84 4.26	42.52 26.46	106.31 66.15	26.58 16.54
$t\bar{t} \to tqh \to \ell\nu bb\bar{b}q$ ILC, 3000 fb^{-1} @ 500 GeV Br($t \to qh$) < 0.112% [12]	Cut MVA	46.20 28.75	115.50 71.86	28.87 17.97	179.44 111.65	448.60 279.13	112.15 69.78
th $\to \ell\nu b\tau^+\tau^-$ LHC, 100 fb^{-1} @ 13 TeV Br($t \to uh$) < 0.15% [13]	Cut MVA	25.75 16.02	64.37 40.05	16.09 10.01	100.01 62.23	250.03 155.58	62.51 38.89
th $\to \ell\nu b\ell^+\ell^- X$ LHC, 100 fb^{-1} @ 13 TeV Br($t \to uh$) < 0.22% [13]	Cut MVA	11.97 7.45	29.92 18.61	7.48 4.65	46.48 28.92	116.20 72.30	29.05 18.08
th $\to jjbb\bar{b}$ LHC, 100 fb^{-1} @ 13 TeV Br($t \to uh$) < 0.36% [13]	Cut MVA	4.47 2.78	11.17 6.95	2.79 1.74	17.35 10.80	43.38 26.99	10.84 6.75

Acknowledgments

This project is supported by the National Natural Science Foundation of China (Grant no. 11675033) and by the Fundamental Research Funds for the Central Universities (Grant no. DUT15LK22).

References

[1] O. Brüning and M. Klein, "The large hadron electron collider," *Modern Physics Letters A*, vol. 28, no. 16, Article ID 1330011, 2013.

[2] M. Klein, "Development of the FCC-he study," in *Proceedings of the FCC Physics, Detector and Accelerator Workshop*, Istanbul, Turkey, March 2016.

[3] C. S. Li, R. J. Oakes, and T. C. Yuan, "QCD corrections to $t \to W^+ \to b$," *Physical Review D*, vol. 43, no. 11, article 3759, 1991.

[4] W.-S. Hou, "Tree level $t \to ch$ or $h \to t^-c$ decays," *Physics Letters B*, vol. 296, pp. 179–184, 1992.

[5] ATLAS Collaboration, "Search for top quark decays $t \to qH$ with $H \to \gamma\gamma$ using the ATLAS detector," *JHEP*, vol. 6, 2014.

[6] ATLAS Collaboration, "Search for flavour changing neutral currents in top quark decays $t \to cH$, with $H \to \gamma\gamma$, and limit on the tcH coupling with the ATLAS detector at the LHC," Tech. Rep. ATLAS-CONF-2013-081, 2013.

[7] V. Khachatryan, A. M. Sirunyan, A. Tumasyan et al., "Searches for heavy Higgs bosons in two-Higgs-doublet models and for $t \to ch$ decay using multilepton and diphoton final states in pp collisions at 8 TeV," *Physical Review D*, vol. 90, no. 11, Article ID 112013, 23 pages, 2014.

[8] J. I. Aranda, A. Cordero-Cid, F. Ramirez-Zavaleta, J. J. Toscano, and E. S. Tututi, "Higgs mediated flavor violating top quark decays $t \to u_iH$, $u_i\gamma$, $u_i\gamma\gamma$ and the process $\gamma\gamma \to tc$ in effective theories," *Physical Review D*, vol. 81, Article ID 077701, 2010.

[9] F. Larios, R. Martinez, and M. A. Perez, "Constraints on top-quark flavor changing neutral couplings from electroweak precision measurements," *Physical Review D*, vol. 72, no. 5, Article ID 057504, 4 pages, 2005.

[10] Y.-B. Liu and Z.-J. Xiao, "Searches for top-Higgs FCNC couplings via the Whj signal with $h \to \gamma\gamma$ at the LHC," *Physical Review D*, vol. 94, no. 5, Article ID 054018, 2016.

[11] L. Wu, "Enhancing thj production from Top-Higgs FCNC couplings," *Journal of High Energy Physics*, vol. 2015, no. 2, article 061, 2015.

[12] H. Hesari, H. Khanpour, and M. M. Najafabadi, "Direct and indirect searches for top-Higgs FCNC couplings," *Physical Review D*, vol. 92, no. 11, Article ID 113012, 2015.

[13] A. Greljo, J. F. Kamenik, and J. Kopp, "Disentangling flavor violation in the top-Higgs sector at the LHC," *JHEP*, vol. 1407, article 46, 2014.

[14] A. Alloul, N. D. Christensen, C. Degrande, C. Duhr, and B. Fuks, "FeynRules 2.0—a complete toolbox for tree-level phenomenology," *Computer Physics Communications*, vol. 185, no. 8, pp. 2250–2300, 2014.

[15] J. Alwall, R. Frederix, S. Frixione et al., "The automated computation of tree-level and next-to-leading order differential cross sections, and their matching to parton shower simulations," *Journal of High Energy Physics*, vol. 2014, no. 7, article no. 079, 2014.

[16] T. Sjöstrand, S. Mrenna, and P. Skands, "PYTHIA 6.4 physics and manual," *Journal of High Energy Physics*, vol. 2006, no. 5, article no. 026, 2006.

[17] J. Pumplin, D. R. Stump, J. Huston, H.-L. Lai, P. Nadolsky, and W.-K. Tung, "New generation of parton distributions with uncertainties from global QCD analysis," *Journal of High Energy Physics*, vol. 2002, no. 7, article no. 012, 2002.

[18] D. Stump, J. Huston, J. Pumplin et al., "Inclusive jet production, parton distributions, and the search for new physics," *Journal of High Energy Physics*, vol. 2003, no. 10, article 046, 2003.

[19] A. Hoecker, P. Speckmayer, J. Stelzer et al., "TMVA—toolkit for multivariate data analysis," PoS ACAT 040, CERN-OPEN-2007-007, 2007.

[20] M. Köksal and S. C. İnan, "Anomalous $tq\gamma$ couplings in γp collision at the LHC," *Advances in High Energy Physics*, vol. 2014, Article ID 935840, 11 pages, 2014.

[21] H. Sun, "Probe anomalous tqγ couplings through single top photoproduction at the LHC," *Nuclear Physics B*, vol. 886, pp. 691–711, 2014.